ELSEVIER

Journal of Chromatography A, 964 (2002) 35–46

JOURNAL OF CHROMATOGRAPHY A

www.elsevier.com/locate/chroma

Study on protein adsorption kinetics to a dye–ligand adsorbent by the pore diffusion model

Songping Zhang, Yan Sun*

Department of Biochemical Engineering, School of Chemical Engineering and Technology, Tianjin University, Tianjin 300072, China

Received 14 November 2001; received in revised form 3 April 2002; accepted 14 May 2002

Abstract

Adsorption kinetics of bovine serum albumin (BSA) and bovine hemoglobin (bHb) to Cibacron Blue 3GA (CB) modified Sepharose CL-6B has been studied. The effects of liquid-phase ionic strength and CB coupling density on the uptake rates of these two proteins in Tris–HCl buffer (pH 7.5) were evaluated by effective pore diffusivity derived from a pore diffusion model. The results showed that despite their similar molecular masses and sizes, the effects of aqueous-phase ionic strength and CB density on the effective pore diffusivities of BSA and bHb were distinctly different. The effective pore diffusivity of BSA to CB-Sepharose increased significantly with decreasing CB density and increasing liquid-phase ionic strength. This was considered due to the decrease in electrostatic repulsion between the BSA and CB molecules of like charge. That is, the increase in ionic strength and the decrease in CB coupling density reduced the electrostatic hindrance effect on BSA diffusion to CB-Sepharose, facilitating the hindered pore diffusion. In contrast, because of the higher isoelectric point of bHb (7.0) compared to BSA (4.7), bHb suffered little electrostatic hindrance effect during its diffusion to CB-Sepharose. Therefore, the effective pore diffusivity of bHb was unchanged with the change in liquid-phase ionic strength and CB coupling density.

Keywords: Kinetic studies; Adsorption; Adsorbents; Pore diffusivity; Mathematical modelling; Ionic strength; Electrostatic interactions; pH effects; Proteins; Albumin; Hemoglobin

1. Introduction

For large-scale affinity chromatography, the triazine dye Cibacron Blue 3GA (CB) linked to agarose beads or other matrices has remarkable advantages over conventional affinity systems [1]. For example, the dye is inexpensive; the coupling procedure is rapid, simple and does not involve the use of toxic chemicals; the dye–ligand adsorbents are stable to biological degradation and have a high capacity for proteins. These properties have established CB-modified agarose as an adsorbent of choice for many large-scale adsorption processes. In order to design and optimize these separation processes, it is necessary to investigate the factors influencing protein adsorption equilibrium and kinetics in detail. It has been well recognized that the liquid-phase ionic strength and CB coupling density have a significant effect on the adsorption equilibria of protein to CB–ligand adsorbents [2–4]. Generally, the adsorption of protein to CB-modified adsorbents increases with decreasing liquid-phase ionic strength and/or increasing coupled ligand density. However,

*Corresponding author. Tel./fax: +86-22-2740-6590.
E-mail address: ysun@tju.edu.cn (Y. Sun).

0021-9673/02/$ – see front matter
PII: S0021-9673(02)00665-9

there is little research dealing with protein adsorption kinetics to the dye–ligand adsorbents.

In contrast to the study on adsorption kinetics of protein to CB–ligand adsorbent, there is considerable experimental information on the diffusion coefficient of proteins and other macromolecules through unmodified agarose gel. It has been reported that the diffusivity of the macromolecules within Sepharose gel was significantly hindered and decreased while protein size increases [5,6]. Studies on the diffusion of globular proteins (serum albumin, ovalbumin and lactalbumin) through SP-Sepharose (6% sulfated agarose gel) of like charge revealed that the transport rate of the proteins increased significantly with increasing ionic strength [7]. This has been considered due to the increased shielding of the repulsive electrostatic interactions [7].

Because several of the aromatic rings in the CB molecule are substituted with negatively charged sulfonate groups, the dye can function as a cation exchanger to bind proteins by electrostatic interactions [8]. On the other hand, however, there would be electrostatic repulsion when the pH value is above the isoelectric point of protein. Therefore, the protein will experience a strong electrostatic exclusion effect when diffusing into the gel at low ionic strength. Furthermore, the electrostatic repulsion should increase with increasing CB coupling density, that is, the surface charge density of the pores. Therefore, the CB coupling density may also give effects on the uptake rate of protein by influencing the electrostatic interaction. Boyer and Hsu [3] studied the kinetics of bovine serum albumin (BSA) to CB-Sepharose CL-6B with a lumped kinetic model and reported that the lumped forward rate constant decreased with increasing dye density. However, there is no report on the effect of liquid-phase ionic strength on the uptake kinetics of protein adsorption to dye–ligand adsorbent.

In this article, two kinds of proteins, BSA and bovine hemoglobin (bHb), which have similar molecular masses and sizes but different isoelectric points, were chosen as model proteins to evaluate the effect of ionic strength, pH and CB coupling density on adsorption kinetics to CB-modified Sepharose CB-6B. The uptake rate of the proteins was analyzed using a pore diffusion model (PDM) incorporated with external film mass transfer, and the dependence of the effective pore diffusivity of the proteins to the CB–ligand adsorbents on liquid-phase ionic strength and CB coupling density was discussed.

2. Materials and methods

2.1. Materials

BSA, bHb and CB were purchased from Sigma (St Louis, MO, USA). The support matrix used was Sepharose CL-6B (Amersham Pharmacia Biotech, Uppsala, Sweden), which has an average particle diameter of 93 μm. All other reagents were of analytical grade.

2.2. Adsorption equilibrium experiments

CB was immobilized to Sepharose CL-6B by the method of He et al. [4]. The dye affinity adsorbents with various levels of CB densities were obtained by varying the initial CB concentration in the coupling reaction [3]. The immobilized CB density was determined spectrophotometrically at 620 nm after digestion of agarose matrix in 1.0 *M* HCl at 80 °C and subsequent neutralization by NaOH [4]. In this work, four affinity adsorbents with CB coupling density ranging from 1.68 to 15.8 μmol/ml were prepared.

A series of adsorption equilibrium experiments of BSA and bHb to CB-Sepharose with different levels of CB substitution were carried out in Tris–HCl buffer (0.01 *M*, pH 7.5). The ionic strength was adjusted by adding a definite amount of NaCl. Another set of adsorption experiments of BSA to CB-Sepharose with CB coupling density of 8.92 μmol/ml were carried out at pH 4.5 and 5.3 in 0.01 *M* NaOAc–0.05 *M* NaCl buffer, and pH 6.5 and 7.5 in 0.01 *M* Tris–HCl–0.05 *M* NaCl buffer. All the adsorption equilibrium experiments were conducted by stirred batch adsorption as described by Zhang and Sun [9]. Generally, about 0.1 ml drained gel, previously equilibrated for 24 h in a proper buffer with a definite ionic strength, was introduced to 10 ml protein solution of known concentration. The suspension was allowed to equilibrate at 25 °C on a shaking incubator at 150 rpm. After 20-h incubation, protein concentration in the supernatant was de-

termined with a UV–Vis spectrophotometer at 280 nm, and the adsorbed density of protein was calculated by mass balance.

2.3. Dynamic adsorption experiments

Dynamic adsorption experiments of BSA and bHb adsorption to CB-Sepharose in Tris–HCl buffer (pH 7.5, 0.01 *M*) containing various NaCl concentrations were performed in a stirred batch system [10]. For BSA, additional kinetic experiments at four different pH values from 4.5 to 7.5 were carried out. In a typical experiment, 1.2 ml of the drained gel was previously equilibrated in 10 ml of a proper buffer with a definite NaCl concentration, and then mixed with 110 ml protein solution in the same buffer with the same ionic strength. The suspension in a flask was mechanically agitated at a speed of about 150 rpm and the temperature was kept at 25 °C with a water bath. Every few minutes, about 3 ml of the liquid was pumped out of the flask through a 1-μm stainless filter to determine the protein concentration. Thereafter, the sample was returned to the vessel immediately. This procedure took less than 0.5 min. By this procedure, the time course of the liquid-phase protein concentration decrease was determined.

2.4. Kinetic model

The adsorption equilibrium data of BSA and bHb to CB-Sepharose under each specific condition were fitted to the Langmuir equation [Eq. (1)] by nonlinear least-squares regression using Origin 5.0 software.

$$q = \frac{q_m c}{K_d + c} \tag{1}$$

The Langmuir equilibrium parameters, q_m and K_d thus obtained were used for adsorption kinetic simulation. The confidence intervals of q_m and K_d predicted by the Origin 5.0 software (95% confidence level) were also obtained (see Tables later).

It is well known that there are at least three discrete steps involved in the protein adsorption from a bulk solution into a solid adsorbent, all of which contribute resistance to protein uptake. These steps include mass transfer from bulk liquid to the outer surface of the particles (film diffusion resistance), movement by diffusion into the pores of the adsorbent (pore diffusion or interior diffusion resistance), and the protein binding to the pore surface (surface reaction resistance) [11]. Though for dye–ligand affinity membrane chromatography, the affinity association kinetics limitation at high flow-rate must be considered when take into account the infinitely fast diffusive mass transfer [12], the adsorption kinetic studies showed that the diffusion of proteins in agarose matrix was rate-limiting in both ion-exchange and biospecific protein adsorption processes when compared to the adsorption reaction [11,13]. The average diffusion time of protein within the gel particle can be approximately calculated by [14]:

$$t_D = \frac{L_D^2}{D_e} \tag{2}$$

where t_D is the diffusion time, L_D is the diffusion path, and D_e is the diffusion coefficient of solute. For the diffusion of protein, such as BSA, within Sepharose CL-6B, L_D can be approximately regarded as the particle radius of Sepharose CL-6B, which is 46.5 μm. The effective pore diffusivity D_e of BSA within Sepharose has been determined to be 5.6×10^{-12} m^2/s at 20 °C [5], or 6.4×10^{-12} m^2/s at 25 °C, corrected using the Stokes–Einstein equation. Taking these parameters into Eq. (2), the time needed for intraparticle diffusion of BSA to Sepharose is estimated at 338 s. For the step of protein binding to the pore surface with CB–ligand, the literature data on the adsorption reaction kinetics suggested that half-times for the binding of protein to dye–ligand adsorbent are around 0.1 s, considerably faster than the speed of the diffusion steps [15,16]. Champluvier and Kula [14] also reported that the adsorption of glucose-6-phosphate dehydrogenase to CB-modified membranes could reach saturation within 1 s. Thus, in this work the protein binding is considered infinitely fast when compared to the intraparticle diffusion, so the concentration of proteins in the adsorbent pore can be assumed in equilibrium with the adsorbed proteins at any radial position, and a pore diffusion model (PDM) incorporating with external film mass transfer [17,18] was employed to describe protein uptake kinetics. In this

model, it is assumed that intraparticle mass transfer occurs by diffusion in liquid-filled pores with a driving force expressed in terms of the pore fluid concentration gradient [17–19]. The mass transfer of protein from liquid phase to solid phase is expressed by:

$$\frac{dc_b}{dt} = -\frac{3k_f H}{r_p}(c_b - c|_{r=r_p}) \quad (3)$$

$$\text{IC: } t = 0,\ c_b = c_{b,0} \quad (3a)$$

The intraparticle continuity equation for the model is described by:

$$\varepsilon_{p,e}\frac{\partial c}{\partial t} + \frac{\partial q}{\partial t} = \frac{D_e}{r^2}\frac{\partial}{\partial r}\left(r^2\frac{\partial c}{\partial r}\right) \quad (4)$$

$$\text{IC: } t = 0,\ c = 0 \quad (4a)$$

$$\text{BC1: } r = 0,\ \frac{\partial c}{\partial r} = 0 \quad (4b)$$

$$\text{BC2: } r = r_p,\ D_e\frac{\partial c}{\partial r} = k_f(c_b - c),\ q = \frac{q_m c}{K_d + c} \quad (4c)$$

In these equations, $\varepsilon_{p,e}$ is the effective particle porosity of Sepharose CL-6B for protein. The values of $\varepsilon_{p,e}$ for BSA and bHb are 0.55 and 0.58, respectively [5]. The film mass transfer coefficient, k_f, is estimated from the following correlation for protein adsorption to adsorbent particles in stirred tank experiments [20]:

$$k_f = \frac{2D_{AB}}{d_p} + 0.31\left(\frac{\mu}{\rho D_{AB}}\right)^{-\frac{2}{3}}\left(\frac{\Delta\rho\mu g}{\rho^2}\right)^{\frac{1}{3}} \quad (5)$$

It should be noted that, although the external mass transfer resistance is included in this model, its effect on the dynamic uptake curves calculated from the model equations is negligible in almost all cases, as is discussed in the next section.

Eqs. (3) and (4), together with the boundary conditions, were solved numerically by the orthogonal collocation method [17] to predict the change in liquid-phase protein concentration with time, and the simulation results were fitted to the dynamic adsorption profile to determine the effective pore diffusivity of protein to CB-Sepharose.

3. Results and discussion

3.1. Effect of liquid-phase ionic strength

The uptake curves of BSA and bHb to CB-Sepharose at different ionic strengths are exhibited in Figs. 1 and 2, respectively. It can be seen that the PDM predicts the dynamic adsorption profiles well. The best fitting values of the effective pore diffusivity (D_e) for BSA and bHb are determined by matching the numerical solution with the experimental data, and the D_e values thus obtained for BSA and bHb are given in Tables 1 and 2, respectively. To examine the effect of the external film mass transfer resistance, the dynamic uptake profile was also fitted by the PDM without considering the external film mass transfer resistance (by setting k_f value as infinity). It was found that the external film mass transfer resistance had little effect on the calculated dynamic adsorption curves of BSA (data not shown).

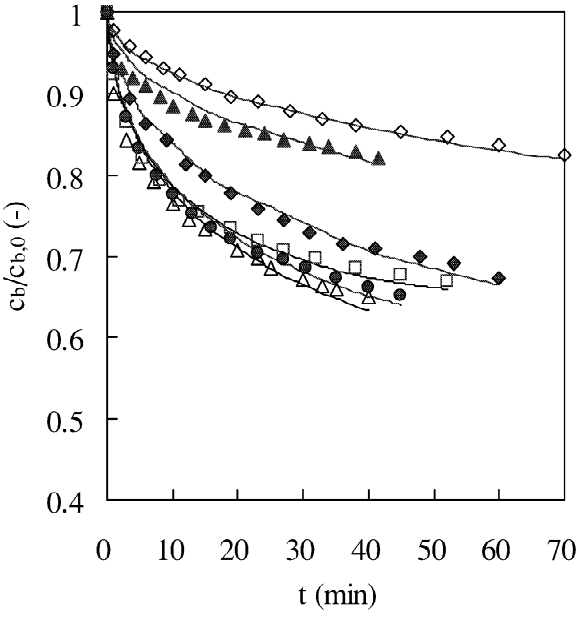

Fig. 1. Experimental and simulated uptake curves of BSA to CB-Sepharose in Tris–HCl buffer (0.01 *M*, pH 7.5) with different ionic strengths. Ionic strengths (*M*): (◇) 0.01; (▲) 0.02; (♦) 0.035; (△) 0.06; (●) 0.085; (□) 0.16. The solid lines are calculated from the PDM. The CB coupling density on CB-Sepharose was 8.92 μmol/ml.

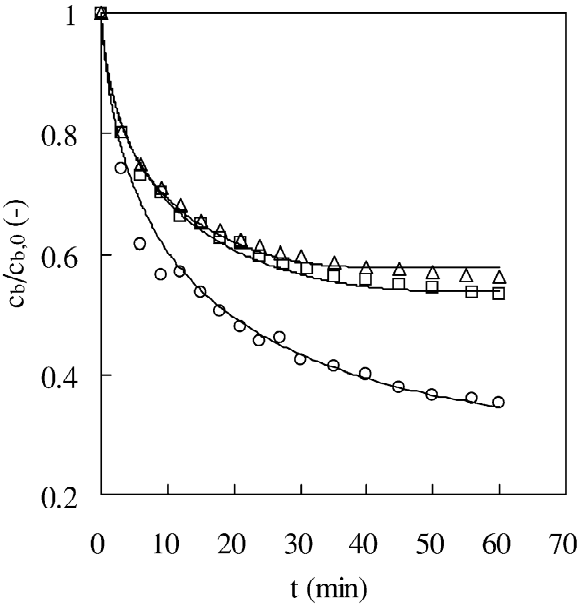

Fig. 2. Experimental and simulated uptake curves of bHb to CB-Sepharose in Tris–HCl buffer (0.01 *M*, pH 7.5) with different ionic strengths. Ionic strengths (*M*): (○) 0.01; (□) 0.02; (△) 0.03. The solid lines are calculated from the PDM. The coupled CB density on CB-Sepharose was 15.8 μmol/ml.

This is attributed to the small D_e values of BSA, that is, the intraparticle diffusion resistance is predominant for the mass transport of BSA. For bHb adsorption kinetics, however, about 16% lower D_e values were obtained when the external film mass transfer resistance was not taken into account in the PDM. This is due to the larger D_e values of bHb than those of BSA. Thus, D_e values predicted by the PDM with external film mass transfer resistance were used for discussion.

The results listed in Tables 1 and 2 suggest that the relationship between adsorption kinetics and ionic strength for BSA and bHb are distinctly different. As can be seen from Fig. 3 (line a) which shows the simulated results for BSA, a slight increase in liquid-phase ionic strength results in a significant increase in the effective pore diffusivity. For example, the value of D_e increased from 0.32×10^{-12} to 1.1×10^{-12} m^2/s while the ionic strength increased from 0.01 to 0.02 *M*. Thereafter, the increase in D_e becomes slower at higher ionic strength. In Fig. 3 (line a), the relationship between D_e and I can be correlated by the following equation with a correlation coefficient of 0.98

Table 1
Parameters of BSA adsorption equilibria and kinetics to CB-Sepharose in Tris–HCl (0.01 *M*, pH 7.5) buffer with different ionic strengths

I (*M*)	$c_{b,0}$ (mg/ml)	H	q_m (mg/ml)	K_d (mg/ml)	D_e (10^{-12} m^2/s)
0.01	1.0	0.01	53.3±1.7	0.127±0.016	0.32
0.02	1.0	0.0075	50.2±1.1	0.042±0.005	1.1
0.035	1.0	0.01	52.7±1.5	0.008±0.002	1.5
0.06	1.0	0.01	52.2±1.4	0.054±0.008	3.8
0.085	1.0	0.01	47.6±0.8	0.070±0.003	4.0
0.16	1.0	0.012	32.4±1.3	0.089±0.022	4.5

CB coupling density was 8.92 μmol/ml; $k_f=4.79\times10^{-6}$ m/s, calculated from Eq. (5).

Table 2
Parameters of bHb adsorption equilibria and kinetics to CB-Sepharose in Tris–HCl (0.01 *M*, pH 7.5) buffer with different ionic strengths

I (*M*)	$c_{b,0}$ (mg/ml)	H	q_m (mg/ml)	K_d (mg/ml)	D_e (10^{-11} m^2/s)
0.01	1.0	0.01	79.3±2.1	0.047±0.005	1.2
0.02	1.0	0.01	49.1±0.9	0.039±0.003	1.1
0.03	1.0	0.01	41.6±0.9	0.033±0.004	1.2

CB coupling density was 15.8 μmol/ml; $k_f=4.95\times10^{-6}$ m/s, calculated from Eq. (5).

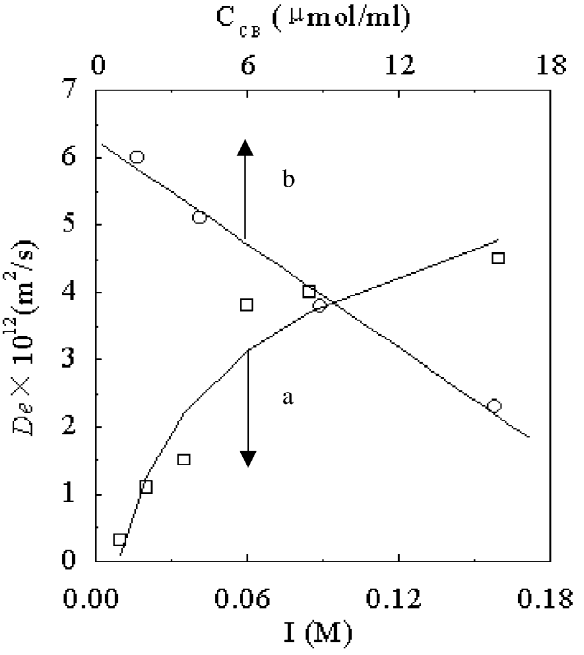

Fig. 3. The dependence of effective pore diffusivity of BSA to CB-Sepharose on liquid-phase ionic strength (line a) and CB coupling density (line b).

$$D_e = \left(\frac{7.66I}{0.04 + I} - 1.40\right) \times 10^{-12} (\mathrm{m^2/s}) \; (I \geq 0.01\, M) \tag{6}$$

From this correlation, it is predicted that D_e will approach 6.26×10^{-12} $\mathrm{m^2/s}$ as ionic strength approaches infinity, which is almost the same as the D_e value of BSA to unsubstituted Sepharose CL-6B determined by Boyer and Hsu [5] after correction using the Stokes–Einstein equation (see above).

In contrast to BSA, the uptake rate of bHb shows little dependence on the liquid-phase ionic strength, as listed in Table 2. Meanwhile, it is notable that the effective pore diffusivity of bHb is much larger than that of BSA although their molecular size is approximately the same (Table 3).

The molecular characteristics of BSA and bHb illustrated in Table 3 suggest that except for the isoelectric point (p*I*), all other properties of BSA and bHb, such as molecular masses, molecular sizes, as well as the diffusion coefficients of the proteins in free solution at 25 °C are similar to each other. Consequently, it is considered that it must be the difference between the isoelectric points of these two proteins that results in the distinctly different dependences of their intraparticle diffusion behaviors on liquid-phase ionic strength.

In a previous report on protein adsorption equilibrium to highly substituted CB-Sepharose (CB density = 15.4 μmol/ml), we have observed that the adsorption of BSA in Tris–HCl buffer (pH 7.5) does not monotonically decrease with increasing liquid-phase ionic strength, but there exists an ionic strength of 0.06 *M* where a maximum BSA adsorption capacity is found [9]. This has been explicitly explained by taking into account the electrostatic interactions between BSA and CB-modified adsorbent of like charge, which decreases with increasing ionic strength (favorable for adsorption), as well as the hydrophobic interaction between CB–ligand and agarose matrix, which increases with increasing ionic strength and therefore decreases the dye–ligand accessible to protein adsorption (unfavorable for adsorption). For the CB-Sepharose with a dye density of 8.92 μmol/ml studied in detail in this paper,

Table 3
Properties of BSA and bHb

Protein	Molecular mass	Dimensions (nm)	Stokes' radius (nm)	p*I*	D_{AB} (10^{-11} $\mathrm{m^2/s}$)
BSA	67 000[a]	4.0×4.0×14.0[c]	3.59[a]	4.7[e]	6.9[f]
bHb	65 000[b]	5.0×5.5×6.4[b]	3.36[d]	7.0[e]	7.2[f]

[a] Data from Ref. [5].
[b] Data from Ref. [21].
[c] Data from Ref. [22].
[d] Calculated from the Stokes–Einstein equation using the literature value of bHb diffusivity at 20 °C [23].
[e] Data from Ref. [24].
[f] Data from Ref. [23] and adjusted to 25 °C according to the Stokes–Einstein equation.

though the change in ionic strength within the range from 0.01 to 0.06 *M* does not result in a significant difference in adsorption capacity of BSA due to the lower dye density, i.e. lower electrostatic repulsion [9], the complex effects of ionic strength leads to the Langmuir dissociation constant showing a non-monotonic trend with ionic strength. As shown in Table 1, the dissociation constant has a minimum value at the ionic strength of 0.035 *M*. Moreover, due to the low p*I* value (4.7) of BSA, there exists electrostatic repulsion between the negatively charged BSA and CB-Sepharose of like charge in Tris–HCl buffer, pH 7.5. At lower ionic strength, the electrostatic repulsion greatly hinders BSA from entering the CB-modified agarose gel; this will greatly affect the uptake rate of BSA adsorption.

According to electrostatic theory, there are diffuse electrical double layers surrounding the charged protein and near to the pore surface of the CB-modified agarose gel. It can be calculated that the Debye length, κ^{-1}, the characteristic length for electrostatic interactions in electrolyte solution, ranges from 3 nm at 0.01 *M* ionic strength to 0.3 nm at 1.0 *M* [9]. Considering the electrostatic repulsion effect, we define an *effective* pore diameter of the gel matrix as follows:

$$d_e = d - 2\kappa^{-1} \quad (I \geq 0.01\ M) \tag{7}$$

where d is the pore diameter of Sepharose CL-6B, and d_e is the *effective* pore diameter for protein to diffuse in. Sepharose CL-6B can be used as a gel filtration medium for the fractionation of proteins from molecular mass 10 000 to 4 000 000, so its pores must be roughly of the same dimensions as proteins [25]. Bosma and Wesselingh [22] reported that the average pore diameter of Sepharose CL-6B was about 35 nm. Considering the pore size distribution, there must be a fraction of relatively small pores, which can be assumed to be, for example, about 10 nm. Thus, at lower ionic strength, the electrical double layers would account for a significant fraction of the interfiber spacing. Taking into account the molecular dimensions of BSA, 4×4×14 nm [22], this electrostatic exclusion would greatly raise the size exclusion of BSA from the gel matrix, intensifying the hindrance effect on BSA transport. By increasing ionic strength, the electrical double layer is compressed, leading to the increase in the *effective* pore diameter for BSA diffusion, thus facilitating the hindered pore diffusion. This effect of ionic strength on the *effective* pore diameter is depicted in Fig. 4. At sufficiently high ionic strength, the electrical double layer will become so thin that it has almost no hindrance effect on BSA diffusion into the matrix. Therefore, the effective pore diffusivity of BSA within CB-Sepharose under this condition should be nearly the same as the D_e value of BSA to an unsubstituted Sepharose CL-6B. As mentioned above, this has been well demonstrated by the D_e value of BSA predicted from Eq. (6) as ionic strength approaches infinity (6.26×10^{-12} m^2/s), which is nearly the same as that of BSA to an unsubstituted Sepharose CL-6B (6.4×10^{-12} m^2/s) [5].

Based on the aforementioned discussion, the liquid-phase ionic strength affects the adsorption kinetics of BSA to CB-Sepharose significantly by altering the electrostatic exclusion between the protein and CB–ligand adsorbent, i.e. the *effective* pore diameter of gel. So it can be anticipated that the protein uptake rate will not depend on ionic strength when there is little electrostatic exclusion between a protein and the CB–ligand adsorbent. This has been well confirmed by the results of bHb adsorption kinetics (Table 2). With higher isoelectric point, i.e. 7.0 [24], bHb carries little negative charge in Tris–HCl buffer (pH 7.5). Therefore, bHb will undergo little electrostatic hindrance effect when its molecules diffuse into the CB-Sepharose gel. As a result, much higher effective pore diffusivity of bHb than

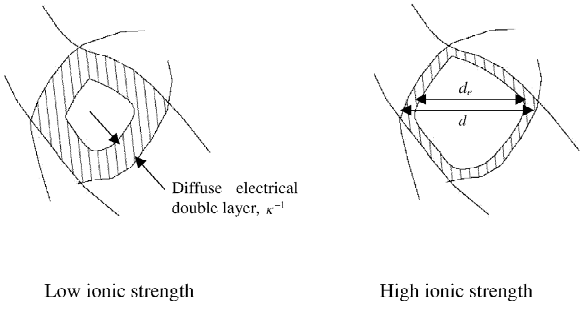

Fig. 4. Schematic explanation for the effect of liquid-phase ionic strength on the *effective* pore diameter of CB-Sepharose for BSA diffusion.

that of BSA to CB-Sepharose was found and the D_e value was unchanged by increasing ionic strength.

3.2. Effect of CB coupling density

The dynamic uptake profiles of BSA to CB-Sepharose with various CB coupling densities are shown in Fig. 5. For each adsorbent, the adsorption kinetics of BSA with initial concentrations of 0.6 and 1.0 mg/ml were studied. The adsorption equilibria parameters fitted by the Langmuir equation and the results of the effective pore diffusivity calculated from the PDM of BSA to CB-Sepharose with different CB coupling densities are summarized in Table 4. The adsorption equilibrium data show that the adsorption capacity increases significantly with increasing CB density, while the dissociation constant does not vary significantly. This result is similar to that observed by Boyer and Hsu [3]. Although some reports on protein adsorption kinetics to an ion exchanger, such

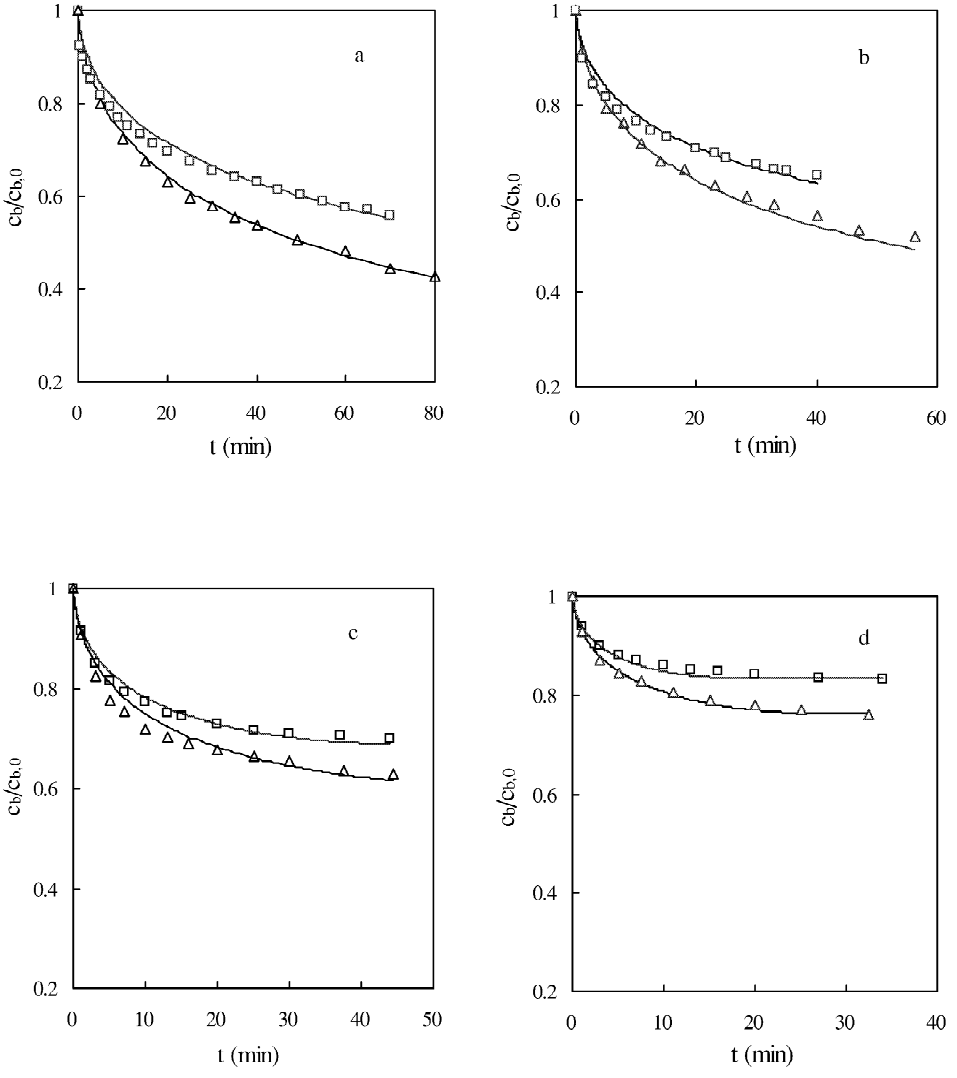

Fig. 5. Experimental and simulated uptake curves of BSA to CB-Sepharose with different CB coupling densities in Tris–HCl buffer (0.01 *M*, pH 7.5) containing 0.05 *M* NaCl. CB densities (μmol/ml): a, 15.8; b, 8.92; c, 4.13; and d, 1.68. Initial BSA concentrations (mg/ml): (□) 1.0; (△) 0.6. The solid lines are calculated from the PDM.

Table 4
Parameters of BSA adsorption equilibria and kinetics to CB-Sepharose with different CB coupling densities in Tris–HCl buffer (0.01 *M*, pH 7.5) containing 0.05 *M* NaCl

C_{CB} (μmol/ml)	$c_{b,0}$ (mg/ml)	H	q_m (mg/ml)	K_d (mg/ml)	D_e (10^{-12} m^2/s)
15.8	1.0	0.01	69.6±1.8	0.038±0.005	2.3
	0.6				2.3
8.92	1.0	0.01	52.2±1.4	0.054±0.008	3.8
	0.6				3.8
4.13	1.0	0.013	25.0±0.8	0.064±0.013	5.1
	0.6				5.1
1.68	1.0	0.013	12.6±0.3	0.050±0.013	6.0
	0.6				6.0

as Poros 50 HS [17] and chitosan-based ion exchanger [26], showed that initial protein concentration had a remarkable effect on the adsorption kinetics, the results listed in Table 4 show that the uptake of BSA by the CB–ligand affinity adsorbent is independent of the initial protein concentration. However, we show here that the D_e value decreased significantly with increasing CB coupling density.

There are two possible reasons for the decrease in D_e with increasing CB density. First, the steric effect by ligand coverage on the CB-Sepharose influences protein diffusion to the adsorbent. Second, as mention above, liquid-phase ionic strength influences BSA diffusion by affecting the electrostatic exclusion of BSA from the adsorbent matrix. Because electrostatic repulsion increases with increasing CB coupling density, that is, the surface charge density of the pores, BSA suffers a larger electrostatic hindrance effect from the CB–ligand adsorbent with higher CB density, leading to smaller effective pore diffusivity.

As a small molecule, the immobilization of CB–ligand should not alter the pore size [25], that is, the steric effect on the protein diffusion might be negligible. Thus, the decrease in the D_e value with increasing CB density would be mainly attributed to the enhancement of electrostatic hindrance effect. As can be seen in Fig. 3 (line b), the relationship between D_e and CB coupling density is linearly related. Simplex fitting gives:

$$D_e = (6.3 - 0.26C_{CB}) \times 10^{-12}\ (m^2/s) \quad (8)$$

This equation was found to regress the experimental data with a correlation coefficient of 0.99. Using this correlation, it can be calculated that the effective pore diffusivity of BSA within an unsubstituted Sepharose CL-6B [i.e. $C_{CB}=0$ in Eq. (8)] is 6.3×10^{-12} m^2/s. As it happens, this value is also approximately the same as the D_e value of BSA to the unsubstituted Sepharose CL-6B (25 °C) determined by Boyer and Hsu [5], as discussed above. Moreover, this value is only slightly larger than the D_e value at a CB density as low as 1.68 μmol/ml (6.0×10^{-12} m^2/s). This implies that at such a low CB density, the electrostatic hindrance effect has become too weak to have a significant effect on protein diffusion.

Boyer and Hsu [3] studied the effect of CB density on the BSA adsorption kinetics to CB-Sepharose CL-6B in fixed-bed chromatography with a lumped kinetic model, and their analysis showed that the lumped forward rate constant decreased with increasing dye density. They ascribed this observation to the difference in binding affinity between protein and CB-Sepharose with different ligand coupling densities. According to the results obtained in this work, however, the electrostatic hindrance effect on protein diffusion is considered to be the main reason for their observation.

The dynamic adsorption curves of bHb to CB-Sepharose with different CB densities were also investigated and the results are shown in Fig. 6. The predicted effective pore diffusivities listed in Table 5 show that the diffusion of bHb has no appreciable

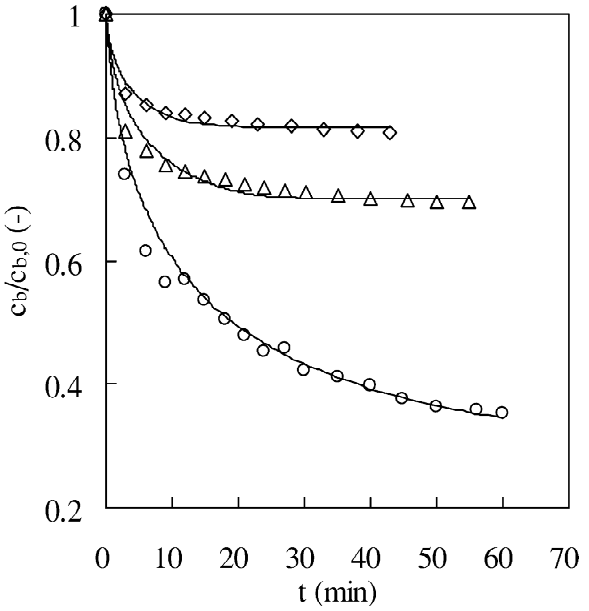

Fig. 6. Experimental and simulated uptake curves of bHb to CB-Sepharose with different CB coupling densities in Tris–HCl buffer (0.01 *M*, pH 7.5). CB coupling densities (μmol/ml): (○) 15.8; (△) 4.13; (◇) 1.68. The solid lines are calculated from the PDM.

dependence on CB density, and these values are the same as those listed in Table 2. Since there are no experimental data available for the effective pore diffusivity of bHb in Sepharose CL-6B in literature, it is calculated using the following correlation for agarose gel proposed by Boyer and Hsu [5]:

$$D_e = 8.34\times10^{-14}\left(\frac{T}{\mu M_w^{1/3}}\right)\exp[-0.1307(M_w^{1/3}+12.45)c_f^{1/2}] \quad (9)$$

where c_f is the polymer fiber concentration of Sepharose CL-6B, which is 0.06. The calculated value from this equation is 1.26×10^{-11} m^2/s for bHb, which is almost the same as those obtained in this work for CB-Sepharose (Tables 2 and 5). This result is in good agreement with what have been discussed above. Because neither steric nor electrostatic hindrance effect exists for bHb diffusion into CB-Sepharose, it is reasonable that the uptake rate of bHb presents no dependence on CB density, and shows the same value as in the unsubstituted Sepharose CL-6B.

3.3. Effect of pH value

To further demonstrate the discussion above on the contribution of electrostatic interactions to BSA diffusion, the effect of pH on the adsorption kinetics of BSA was studied. It has been reported that the BSA molecule remains in heart-shaped conformation in solution in the pH range from 4.5 to 8.0 [27], while at pH values below 4, it undergoes an irreversible structural transition that affects adsorption behavior [28]. Therefore, in this work, we chose pH values of 4.5–7.5 to investigate the effect of pH. The dynamic adsorption curves of BSA to CB-Sepharose under different pH values are shown in Fig. 7. As listed in Table 6, little dependence of BSA diffusivity on pH can be found except for a slightly higher value at pH 4.5.

This result is apparently contradictory to the ionic-strength dependence of BSA diffusivity, since the net charges of BSA would change greatly in the pH range, leading to the change in the electrostatic interactions between the BSA molecule and the gel surface. However, this inconsistency can be explained as follows: (1) Although the net negative charges of BSA increase with increasing pH, the electrical double layer on the gel surface is little affected by pH. That is, the charge density on the gel surface or the *effective* pore diameter does not vary

Table 5
Parameters of bHb adsorption equilibria and kinetics to CB-Sepharose with different CB densities in Tris–HCl buffer (0.01 *M*, pH 7.5)

C_{CB} (μmol/ml)	$c_{b,0}$ (mg/ml)	H	q_m (mg/ml)	K_d (mg/ml)	D_e (10^{-11} m^2/s)
15.8	1.0	0.01	79.3±2.1	0.047±0.005	1.2
4.13	1.0	0.01	36.1±2.6	0.166±0.039	1.2
1.68	1.0	0.01	32.7±3.8	0.682±0.195	1.2

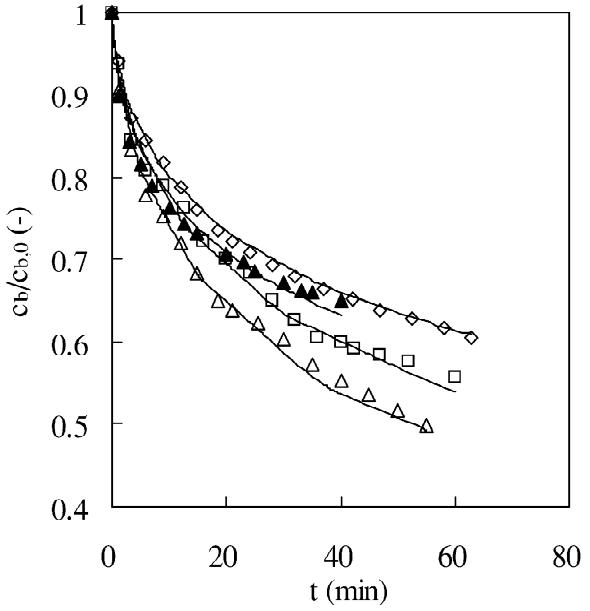

Fig. 7. Experimental and simulated uptake curves of BSA to CB-Sepharose under different pH values. pH values: (△) 4.5; (□) 5.3; (◇) 6.5; (▲) 7.5. The solid lines are calculated from the PDM.

with pH. Therefore, the electrostatic hindrance effect on BSA diffusion does not change with pH. (2) It has been well known that BSA molecules favorably bind negative charges like Cl^- involved in this work [29]. Thus, the BSA molecule would carry additional negative charges besides its intrinsic charges. Bosma and Wesselingh [22] have reported that the net charge of BSA in acetate and Tris buffers of 25 m*M* ranged from −5 to −15 in the pH range of 4.5–7.5. The results indicate that in the pH range we studied, the BSA molecules carry negative charges, and would encounter an electrostatic hindrance effect during its diffusion in the CB-Sepharose gel. Although the net negative charges increase with increasing pH value, it would not give an additional electrostatic hindrance effect on protein diffusion. Hence, it is considered that the independence of BSA diffusivity on pH is reasonable.

4. Conclusions

It has been shown that liquid-phase ionic strength and CB coupling density gave a significant effect on BSA adsorption kinetics to CB-modified Sepharose CL-6B in Tris–HCl buffer pH 7.5. The effective pore diffusivity of BSA to CB-Sepharose derived from the PDM increased significantly with increasing ionic strength within the ionic strength range studied (0.01–0.16 *M*). On the other hand, the effective pore diffusivity decreased linearly with increasing CB density. These results have been elucidated by considering the electrostatic repulsions between BSA and CB molecules of like charge. Increasing ionic strength or decreasing CB density decreased the electrostatic hindrance effect for BSA resulting from the electrostatic repulsion, and thus facilitating the hindered pore diffusion. In contrast, although with similar molecular mass and size, the effective pore diffusivity of bHb was unchanged with changing liquid-phase ionic strength and CB density. This was due to the higher isoelectric point of bHb (p*I* 7.0) than that of BSA (4.7); little electrostatic hindrance effect existed for bHb diffusion to the CB-Sepharose in Tris–HCl buffer pH 7.5. Therefore, the variation in liquid-phase ionic strength and CB density did not result in appreciable changes in the effective pore diffusivity of bHb. The study on the adsorption kinetics of BSA to CB-Sepharose under various pH values showed that there is little dependence of effective pore diffusivity on pH values.

Table 6
Parameters of BSA adsorption equilibria and kinetics to CB-Sepharose at different pH values

pH	$c_{b,0}$ (mg/ml)	H	q_m (mg/ml)	K_d (mg/ml)	D_e (10^{-11} m^2/s)
4.5	1.0	0.0075	106.6±3.5	0.0026±0.0008	4.0
5.3	1.0	0.0075	87.0±2.1	0.0072±0.0022	3.8
6.5	1.0	0.0075	65.9±1.7	0.025±0.004	3.8
7.5	1.0	0.01	52.2±1.4	0.054±0.008	3.8

CB coupling density was 8.92 μmol/ml.

5. Nomenclature

c	Protein concentration in pore (mg/ml)
c_b	Bulk phase protein concentration (mg/ml)
$c_{b,0}$	Initial bulk phase protein concentration (mg/ml)
c_f	Polymer fiber concentration in Sepharose CL-6B (-)
C_{CB}	CB coupling density (μmol/ml)
d	Pore diameter of Sepharose CL-6B (m)
d_e	Effective pore diameter defined by Eq. (7) (m)
d_p	Mean particle diameter (m)
D_{AB}	Molecular diffusivity of protein in free solution (m^2/s)
D_e	Effective pore diffusivity (m^2/s)
g	Gravitational constant ($=9.81\ m/s^2$)
H	Volume ratio of solid to liquid phases (–)
I	Ionic strength (M)
K_d	Dissociation constant for the Langmuir isotherm (mg/ml)
k_f	Liquid film mass transfer coefficient (m/s)
L_D	Mean diffusion path (m)
M_w	Molecular mass (D)
q	Adsorbed protein density in equilibrium with c (mg/ml)
q_m	Adsorption capacity for the Langmuir isotherm (mg/ml)
r	Radial distance (m)
r_p	Mean particle radius (m)
t	Time (s)
t_D	Average diffusion time of protein within Sepharose CL-6B particle (s)
T	Temperature (K)
$\varepsilon_{p,e}$	Effective intraparticle porosity for protein (–)
κ^{-1}	Debye length (m)
μ	Liquid viscosity (Pa s)
ρ	Liquid density (kg/m^3)
$\Delta\rho$	Density difference between solid and liquid phases (kg/m^3)

Acknowledgements

This work was supported by the National Natural Science Foundation of China (grant no. 20025617).

References

[1] T. Atkinson, P.M. Hammond, R.D. Hartwell, P. Hughes, M.D. Scawen, R.F. Sherwood, D.A.P. Small, C.J. Bruton, M.J. Harvey, C.R. Lowe, Biochem. Soc. Trans. 9 (1981) 290.
[2] P.M. Boyer, J.T. Hsu, Biotechnol. Tech. 4 (1990) 61.
[3] P.M. Boyer, J.T. Hsu, Chem. Eng. Sci. 47 (1992) 241.
[4] L.Z. He, Y.R. Gan, Y. Sun, Bioprocess Eng. 17 (1997) 301.
[5] P.M. Boyer, J.T. Hsu, AIChE J. 38 (1992) 259.
[6] M. Moussaoui, M. Benlyas, P. Wahl, J. Chromatogr. 591 (1992) 115.
[7] E.M. Johnson, D.A. Berk, R.K. Jain, W.M. Deen, Biophys. J. 66 (1995) 1561.
[8] R.K. Scopes, Anal. Biochem. 165 (1987) 235.
[9] S.P. Zhang, Y. Sun, Biotechnol. Bioeng. 75 (2001) 710.
[10] L.Z. He, X.Y. Dong, Y. Sun, Biochem. Eng. J. 2 (1998) 53.
[11] B.J. Horstmann, H.A. Chase, Chem. Eng. Res. Des. 67 (1989) 243.
[12] K.G. Briefs, M.R. Kula, Chem. Eng. Sci. 47 (1992) 141.
[13] G.L. Skidmore, B.J. Horstmann, H.A. Chase, J. Chromatogr. 498 (1990) 113.
[14] B. Champluvier, M.R. Kula, Biotechnol. Bioeng. 40 (1992) 33.
[15] A.F. Bergold, D.A. Hanggi, A.J. Muller, P.W. Carr, in: Cs. Horvath (Ed.), High Performance Liquid Chromatography, Academic Press, New York, 1988.
[16] D.K. Schisla, Ph.D. Thesis, University of Minnesota, 1990.
[17] L.E. Weaver, G. Carta, Biotechnol. Prog. 12 (1996) 342.
[18] B. Xue, Y. Sun, J. Chromatogr. A 921 (2001) 109.
[19] P.R. Wright, F.J. Muzzio, B.J. Glasser, Biotechnol. Prog. 14 (1998) 913.
[20] C.J. Geankopolis (Ed.), Transport Processes and Unit Operations, 2nd ed., Allyn and Bacon, New York, 1983.
[21] H. Shirahama, K. Suzuki, T. Suzawa, J. Colloid. Interf. Sci. 129 (1989) 483.
[22] J.C. Bosma, J.A. Wesselingh, AIChE J. 44 (1998) 2399.
[23] M.T. Tyn, T.W. Guesk, Biotechnol. Bioeng. 35 (1990) 327.
[24] J.Y. Yoon, J.H. Lee, J.H. Kim, W.S. Kim, Colloids Surface B Biointerfaces 10 (1998) 365.
[25] B.J. Horstmann, C.N. Kenney, H.A. Chase, J. Chromatogr. 361 (1986) 179.
[26] H. Yoshida, M. Yoshikawa, T. Kataoka, AIChE J. 40 (1994) 2034.
[27] D.C. Carter, J.X. Ho, in: Advances in Protein Chemistry, Academic Press, New York, 1994.
[28] V. Bloomfield, Biochemistry 5 (1996) 684.
[29] G. Scatchard, W.T. Yap, J. Am. Chem. Soc. 86 (1964) 3434.